

Impact of Metrology on the Evaluation of Advanced eGaN FET Power Converters

Rushi Patel and Benjamin Kromann
Department of Electrical and Computer Engineering
Mississippi State University
Starkville, MS 39762

Faculty Advisor: Michael S. Mazzola

Abstract

An advanced semiconductor device applications research program at Mississippi State University is exploring measurement methods appropriate for high-efficiency, high-frequency power conditioning systems. In the evaluation of any electronic device, the measurement methods used will have an impact on the reliability of the collected data. This becomes more relevant when dealing with high-efficiency, high-frequency devices. The specific topic of this paper details the application and performance evaluation of an enhancement-mode Gallium Nitride field-effect transistor (eGaN FET) in a buck converter operating at several switching frequencies extending into the megahertz band. Advancements in wide band-gap power semiconductor devices (of which the eGaN FET is one) have resulted in dramatic increases in efficiency and system bandwidths as compared to their silicon counterparts. The former advancement leads to increasingly low power loss, which is harder to accurately measure and quantify. The later advancement has pushed operating frequencies into the megahertz spectrum. This means that the time period between high and low levels is extremely short, resulting in fewer data points per period. Conventional measurement methods in this application may result in measurement errors brought about by electromagnetic interference, lack of precision and inherent system losses. For power and efficiency measurements, a synthetic four-point measurement is adopted using four 6.5-digit multi-meters. Kelvin connected voltage measurements are made at the input and output terminals of the system. Similarly, precision shunt measurements capture DC input and output currents. Additionally, a giga-sample capable oscilloscope captures any ripple voltages and currents using compensated high impedance 10x attenuated probes. True RMS values of all voltage and current measurements are calculated in post-process computations. These results are compared against data captured using simpler yet less precise conventional means to fully document the effect that appropriate measurement method has on the evaluation of devices of this nature.

Keywords: Power Electronics, Gallium Nitride Transistor, Precision Metrology

1. Introduction

Metrology is the scientific study of measurement. The most important parameter in metrology, and therefore in the distinction between measurement methods, is precision. In general, better measurement methods entail more precision.

One very important factor of a DC-DC converter's performance is its efficiency, and this is the focus of its characterization and analysis. This will yield how much power is lost in the conversion from one DC value to the other. This value helps to give a clear picture of what is going on inside the converter and how efficiency could be improved through design modifications.

This is all dependent, of course, on how precise the measurement methods for input and output power values are. As discussed later, a difference in precision can make a very large difference in the results of an efficiency characterization, and whether data is useful for analysis at all.

As for the experimenters' choice of platform, GaN is a relatively newly-adopted power transistor material which has several interesting characteristics that prove to be significantly beneficial for switch-mode power converters. GaN devices, when compared to Silicon or even Silicon Carbide, have lower on resistance, leading to lower conduction loss; faster switching, leading to lower switching loss; and less parasitic capacitance, leading to less losses in charging and discharging. GaN is also proportionally much smaller than its other device counterparts. All these factors lead to increased performance in several switch-mode power converter applications.

The primary reason eGaN provides a great platform on which to test this concept is that GaN FET converters are known to be very efficient within their optimal operating range. As the efficiency approaches 100%, it becomes more important that the measurement be precise, so that any informed conclusions can be drawn about what losses are still present, among other things.

2. Methods and Analysis

Two different Analysis methods were used to validate the results and make appropriate conclusions: Experimental Analysis and Theoretical Analysis.

2.1 Experimental Analysis

This experiment used the EPC 9036 eGaN half bridge DC-DC synchronous buck converter development board. This development board allowed freedom to choose appropriate filter components to stabilize the system. A combination of a 270nH inductor and a 10 μ F capacitor were chosen for the filter.

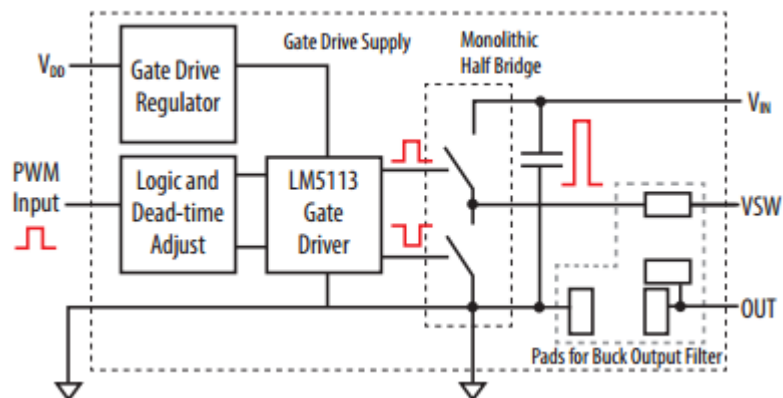


Figure 1: EPC 9036 development board block diagram [1].

A block diagram of the buck converter is shown in Figure 1. A 12V DC power supply was connected to the input voltage (V_{in}). To turn on the eGaN transistors, the pulse width modulation (PWM) input was set to duty ratio of 10%, 20%, and 30% for three different cases. A function generator with an amplitude of 3V peak to peak and a frequency of 1MHz generated the PWM waveform. A 10V DC power supply was connected to the VDD terminal to provide power to run the LM5113 gate driver. This gate drive is designed to drive GaN FETs in a synchronous buck or a half bridge configuration.

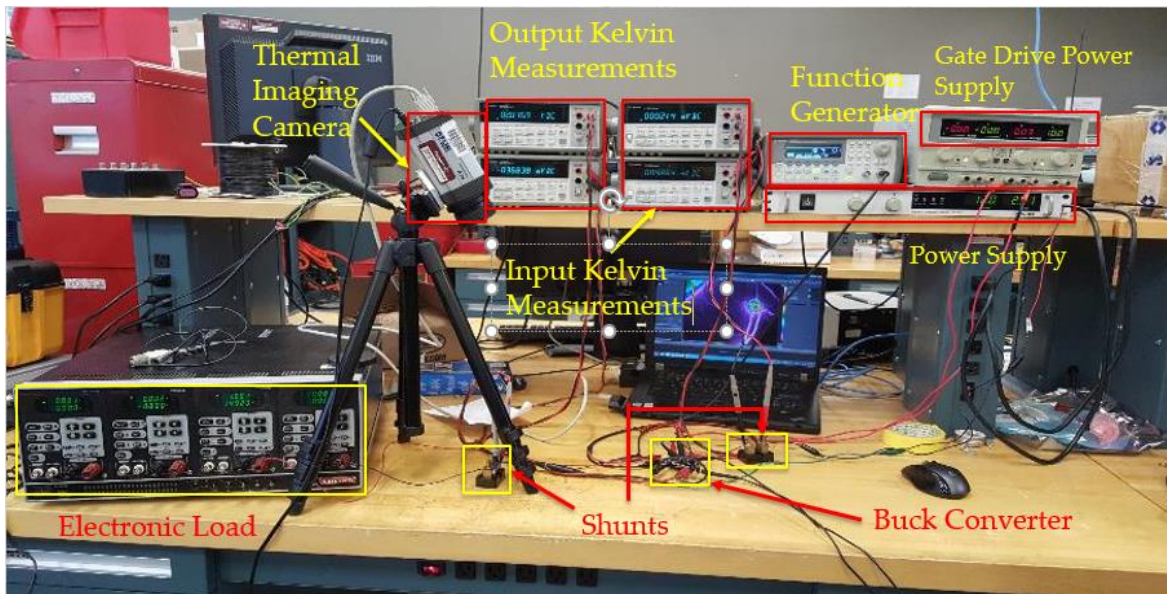


Figure 2: Experimental setup

The experimental setup included four 6.5-digit multi-meters, a function generator, two DC power supplies, a thermal imaging camera, shunt resistances, and the development board - as shown in Figure 2. The electronic load was used to obtain desired output current over a set range of test values. Two of the multimeters measured the input voltage and current while other two measured the output voltage and current to calculate the overall efficiency. The thermal imaging camera was useful to determine the power loss due to heat dissipation, as well as to track the temperature rise to determine when the converter had reached thermal equilibrium. Constant monitoring of the thermal imaging camera assisted in deriving a new equation for the conduction loss of the eGaN FET, which is discussed in detail in theoretical analysis.

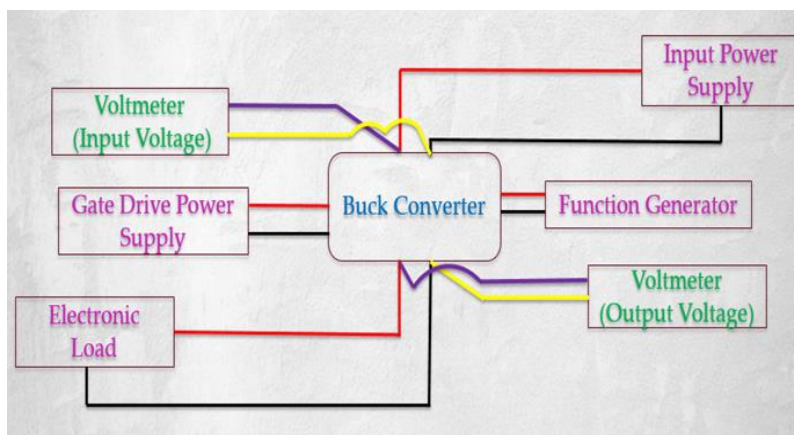


Figure 3: Simple metrology diagram

In this study, emphasis was put on the measurements of the input and output current by implementing two different measurement methods. The first, shown in Figure 3, is a more simplistic method widely used by hobbyists and undergraduate students to derive values for simple calculations for circuit analysis or testing. This simple method relies on imprecise measurement of current, which has a distinct effect on the measurement of power, and, consequently, power efficiency. In this method, a synthetic kelvin connected measurement was utilized to measure the input and output voltages directly from the buck converter. However, the input and output current measurements were taken directly from the input power supply and the electronic load.

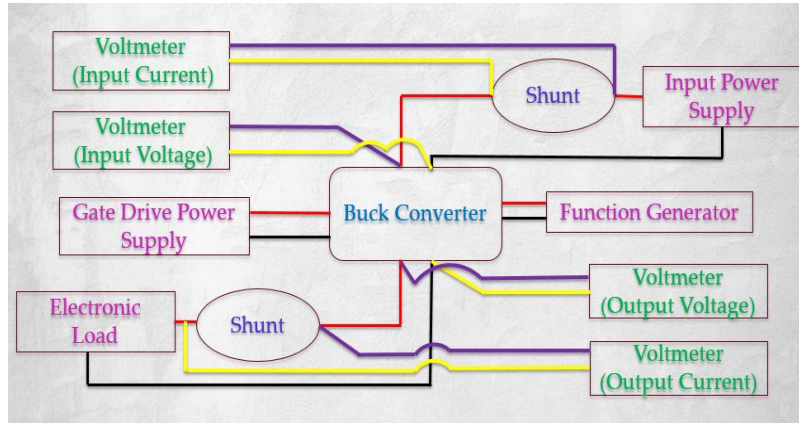


Figure 4: Precise metrology diagram

The second method, shown in Figure 4, is a more precise method, which is utilized in industry applications of power converter characterization. It alleviates the problems incurred by the simple method by relying on extremely precise shunt resistances and derivative calculation to provide much better current values. Similar to the simple method, this method measured the input and output voltage directly from the board using kelvin connected measurements. However, shunt resistances were placed in series to both the input power supply and the electronic load to derive precise measurement of input and output currents.

2.2 Theoretical Analysis

To calculate the efficiency theoretically, the different power losses of the buck converter were evaluated. The various power loss equations were obtained from application notes published by Fairchild and Texas Instruments [2-4]. These power losses included the losses inherent in the eGaN FET module as well as the inductor loss, capacitor loss, etc. All the examined losses are listed below:

High Side (HS) and Low Side (LS) conduction losses are given by equations (1) and (2) respectively:

$$P_{cond(HS)} = R_{ds(ON)HS} * I_{RMS(HS)}^2 \quad (\text{Eq. 1})$$

$$P_{cond(LS)} = (R_{ds(ON)LS} * \left(\frac{(2.706 * I_{RMS(LS)} + 23)}{25} \right)^2) * I_{RMS(LS)}^2 \quad (\text{Eq. 2})$$

$$I_{RMS(HS)} = \sqrt{\frac{D}{3} * \left(\left(I_{out} + \frac{I_{ripple}}{2} \right)^2 + \left(I_{out} + \frac{I_{ripple}}{2} \right) * \left(I_{out} - \frac{I_{ripple}}{2} \right) + \left(I_{out} - \frac{I_{ripple}}{2} \right)^2 \right)} \quad (\text{Eq. 3})$$

$$I_{RMS(LS)} = \sqrt{\frac{1-D}{3} * \left(\left(I_{out} + \frac{I_{ripple}}{2} \right)^2 + \left(I_{out} + \frac{I_{ripple}}{2} \right) * \left(I_{out} - \frac{I_{ripple}}{2} \right) + \left(I_{out} - \frac{I_{ripple}}{2} \right)^2 \right)} \quad (\text{Eq. 4})$$

$$I_{ripple} = \frac{(V_{in} - V_{out}) * D * T_{sw}}{L} \quad (\text{Eq. 5})$$

During operation, the LS eGaN transistor experienced deadtime, resulting in Deadtime loss, which can be calculated by equation (6). The gate drive loss is given by equation (7).

$$P_{deadtime} = V_{SD} * \left(\left(I_{out} - \frac{I_{ripple}}{2} \right) * t_{deadtime(rise)} + \left(I_{out} - \frac{I_{ripple}}{2} \right) * t_{deadtime(rise)} \right) * f_{sw} \quad (\text{Eq. 6})$$

$$P_{gate} = P_{gate(HS)} + P_{gate(LS)} = (Q_{g(HS)} + Q_{g(LS)}) * V_{driver} * f_{sw} \quad (\text{Eq. 7})$$

$$t_{deadtime(rise)} \approx t_{delay(rise)} \quad (\text{Eq. 8})$$

$$t_{deadtime(fall)} = t_{delay(fall)} + \frac{Q_{gs(LS)} * (R_{gate} + R_{driver})}{V_{driver} - \frac{V_{th}}{2}} \quad (\text{Eq. 9})$$

LS switching loss is neglected due to super-soft switching at normal operation. HS switching loss is given by equation (10):

$$P_{sw(HS)} = V_{in} * I_{out} * f_{sw} * \frac{Q_{sw}}{I_g} \quad (\text{Eq. 10})$$

$$I_g = \frac{V_{driver} - V_{PL}}{R_g + R_{driver}} \quad (\text{Eq. 11})$$

DC Resistance (DCR) in the inductor and Equivalent Series Resistance (ESR) in the capacitor were directly proportional to the inductor and capacitor loss. Capacitor loss and inductor loss is given by equation (12) and equation (13) respectively:

$$P_{DCC} = I_{ripple}^2 * ESR \quad (\text{Eq. 12})$$

$$P_{DCL} = I_{RMS(L)}^2 * DCR \quad (\text{Eq. 13})$$

$$I_{RMS(L)} = \sqrt{I_{out}^2 + \frac{I_{ripple}^2}{12}} \quad (\text{Eq. 14})$$

The output capacitance loss for HS and LS is given by equation (15) and equation (16) respectively:

$$P_{Coss(HS)} = 0.5 * Q_{oss(HS)} * V_{in}^2 * f_{sw} \quad (\text{Eq. 15})$$

$$P_{Coss(LS)} = 0.5 * Q_{oss(LS)} * V_{in}^2 * f_{sw} \quad (\text{Eq. 16})$$

Table I. Parameters and Values

Parameter	Value	Parameter	Value	Parameter	Value
V_{in}	12V	$R_{ds(ON)LS}$	1.5m Ω	$t_{delay(fall)}$	750ps
V_{out}	1.2V	V_{driver}	10V	$Q_{gs(LS)}$	4.6nC
R_{gate}	0.3 Ω	ESR	1.5m Ω	V_{th}	1.2V
C	10 μ F	R_{driver}	2.7 Ω	V_{sd}	1.8V
f_{sw}	1MHz	$Q_{sw(HS)}$	1.1nC	R_{gate}	0.3 Ω
T_{sw}	1 μ s	$Q_{g(HS)}$	3.5nC	$C_{oss(LS)}$	1600pF
$C_{oss(HS)}$	290pF	I_{out}	0A to 32A	DCR	.29m Ω
$R_{ds(ON)HS}$	6m Ω	$t_{delay(rise)}$	650ps	$Q_{g(LS)}$	15nC

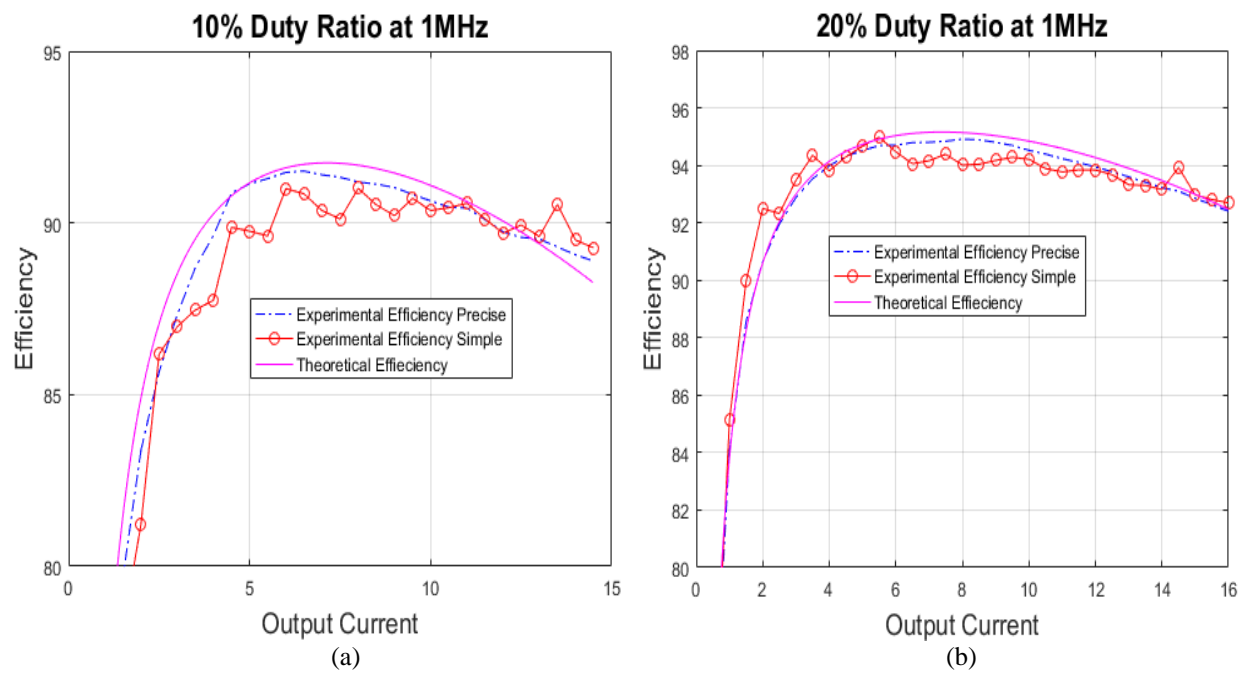
All the parameters used in the equations from (1) to (16) are provided in Table I. The parameters are obtained from datasheets of the eGaN transistor EPC 2100 as well as Coilcraft and Yageo [5-7]. To calculate the total loss, all individual losses were added together. The product of output current and output voltage gave the output power. Input

power was calculated by adding output power to total loss. Finally, efficiency was obtained from dividing input power by output power.

MATLAB software was utilized to avoid complexity of calculating equations by hand [8]. One of its unique features is to allow variables to be defined in a range. With increments of 0.032, the output current was defined from 0 to 32 amps to ensure a precise efficiency curve. The efficiency data was taken at a frequency of 1MHz with 10%, 20%, and 30% duty ratios.

3. Results and Discussion

The theoretical efficiency was obtained with the help of MATLAB. This theoretical data included one thousand points and was plotted in a graph to make a comparison with the empirical data for both measurement methods. Plots are shown in Figure 5.



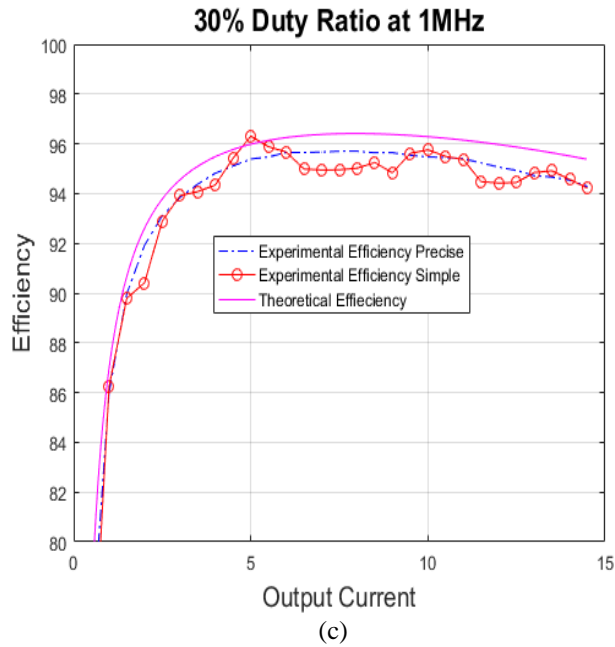


Figure 5: Output Current Vs Efficiency at 1 MHz for duty ratio of: (a) 10%, (b) 20%, and (c) 30%.

It can be clearly seen that using the simple method to obtain experimental efficiency data produces a very uneven graph and has sudden unexpected changes, making it less comparable with the theoretical efficiency data. On the other hand, the data yielded by the precise method produces no oscillation and shows instead a very smooth curve, directly comparable with the theoretical efficiency data. Even though the precise method does not exactly match the theoretical efficiency data, the difference between the two is less than 1%.

4. Conclusion

This research demonstrates several relevant characteristics of power converters and their characterization, especially with regards to metrology. First, the data shows a significant difference between the simple measurement method and the precise measurement method in how close the experimental data mirrors the theoretical. Second, the theoretical model, calculated using all known power losses within a typical buck converter, does very well at predicting the efficiency of an eGaN FET power converter like the one used here. Thirdly, the data at extremely high efficiencies (such as near 96%) shows some very slight, proportional disparity between experimental and theoretical data. This indicates that there may be small, unknown losses at that high efficiency.

The reason this can be inferred at all is based upon the fidelity of the measurements used. Without attention to metrology, a theoretical model can never be evaluated to the degree that it needs to be, in many applications. This is especially true about high efficiency power converters such as the eGaN FET buck converter analyzed here.

5. Acknowledgements

This work was supported primarily by the Center for Advanced Vehicular Systems (CAVS) at Mississippi State University. We would also like to thank my faculty advisor Dr. Michael S. Mazzola and Mr. Jim Gafford for his ideas and support throughout this research project.

6. References

[1] Efficient Power Conversion. (2014). *Development Board EPC9036 Quick Start Guide*. [Online]. Available: http://epc-co.com/epc/Portals/0/epc/documents/guides/EPC9036_qsg.pdf

- [2] Jon Klein. (2014, November 21). *Synchronous buck MOSFET loss calculations with Excel model*. [Online]. Available: <https://www.fairchildsemi.com/application-notes/AN/AN-6005.pdf>
- [3] David Jauregui, Bo Wang, Rengang Chen. (2011, July). *Power Loss Calculation with Common Source Inductance Consideration for Synchronous Buck Converters*. [Online]. Available: <http://www.ti.com/lit/an/slpa009a/slpa009a.pdf>
- [4] Brigitte Hauke. (2015, August). *Basic Calculation of a Buck Converter's Power Stage*. [Online]. Available: <http://www.ti.com/lit/an/slva477b/slva477b.pdf>
- [5] Efficient Power Conversion. (2015, April). *EPC2100 – Enhancement Mode GaN Power Transistor Half Bridge Preliminary Specification Sheet*. [Online]. Available: http://epc-co.com/epc/Portals/0/epc/documents/datasheets/EPC2100_preliminary.pdf
- [6] Coilcraft. (2016, June 1). *Shielded Power Inductors – SLR1070*. [Online]. Available: <http://www.coilcraft.com/pdfs/slr1070.pdf>
- [7] Yageo. (2016, January 28). *Surface Mount Multilayer Ceramic Capacitors*. [Online]. Available: http://www.yageo.com/documents/recent/UPY-GPHC_X5R_4V-to-50V_24.pdf
- [8] MathWorks. (2016). *Global Optimization Toolbox: User's Guide (R2016a)*. [Online]. Available: http://www.mathworks.com/help/pdf_doc/gads/gads_tb.pdf